Molecular Human Reproduction, Vol. 0, No. 0 pp. 1–13, 2014
Mol. Hum. Reprod. Advance Access published March 20, 2014
doi:10.1093/molehr/gau015

molecular human reproduction
MHR | basic science of reproductive medicine

ORIGINAL RESEARCH

Gene expression in human ovarian tissue after xenografting

A. Van Langendonckt[1], L. Romeu[1], J. Ambroise[2], C. Amorim[1], B. Bearzatto[2], J.L. Gala[2], J. Donnez[3], and M.M. Dolmans[1,*]

[1]Pôle de Recherche en Gynécologie, Institut de Recherche Expérimentale et Clinique, Université Catholique de Louvain, B-1200 Brussels, Belgium [2]Centre de Technologies Moléculaires Appliquées, Institut de Recherche Expérimentale et Clinique, Université Catholique de Louvain, B-1200 Brussels, Belgium [3]Société de Recherche pour l'Infertilité (SRI), B-1150 Brussels, Belgium

*Correspondence address. Department of Gynecology, Université Catholique de Louvain, Cliniques Universitaires St Luc, Avenue Mounier 52, B1.52.02, 1200 Brussels, Belgium. Tel: +32-2-764-52-87; Fax: + 32-2-764-95-07; E-mail: marie-madeleine.dolmans@uclouvain.be, anne.lepage@uclouvain.be

Submitted on September 4, 2013; resubmitted on February 18, 2014; accepted on February 24, 2014

ABSTRACT: Cryobanking and transplantation of ovarian tissue is a promising approach to restore fertility in cancer patients. However, ischemic stress following avascular ovarian cortex grafting is known to induce stromal tissue fibrosis and alterations in follicular development. The aim of the study was to analyze the impact of freeze-thawing and grafting procedures on gene expression in human ovarian tissue. Frozen–thawed ovarian tissue from 14 patients was xenografted for 7 days to nude mice and one ungrafted fragment was used as a control. Immediately after recovery, grafts were processed for RNA extraction and histological analysis. Their expression profile was screened by whole-genome oligonucleotide array ($n = 4$) and validated by reverse-transcriptase polymerase chain analysis ($n = 10$). After data filtering, the Limma package was used to build a linear regression model for each gene and to compute its fold change between tissues on Days 0 and 7. After adjusting the *P*-value by the Sidak method, 84 of the transcripts were significantly altered after 7 days of grafting, including matrix metalloproteinase-9 and -14 and angiogenic factors such as placental growth factor and C-X-C chemokine receptor type 4 (CXCR4). Major biological processes were related to tissue remodeling, including secretory processes, cellular adhesion and response to chemical and hormonal stimuli. Angiopoietin signaling, the interleukin-8 pathway and peroxisome proliferator-activated receptor activation were shown to be differentially regulated. On Day 7, overexpression was confirmed by PCR for interleukin-8, transforming growth factor-beta 1, matrix metalloproteinase-14 and CXCR4, compared with ungrafted controls. In conclusion, new as well as known genes involved in tissue restructuring and angiogenesis were identified and found to play a key role during the first days after human ovarian tissue transplantation. This will facilitate the development of strategies to optimize grafting techniques.

Key words: human ovarian tissue / gene expression / microarray / transplantation / ischemic stress

Introduction

Recent progress in cancer therapies has significantly increased long-term survival rates in patients. Unfortunately, these treatments can be very harmful to the ovaries, resulting in loss of both endocrine and reproductive functions in women (Wallace *et al.*, 2005; Donnez *et al.*, 2006). Cryopreservation and transplantation of ovarian tissue is now offered in an increasing number of reproductive medicine centers to preserve fertility of cancer patients in cases where embryo or oocyte cryopreservation cannot be applied. Since the birth of the first baby after orthotopic transplantation of frozen–thawed ovarian tissue (Donnez *et al.*, 2004), 24 live births have been reported (Donnez *et al.*, 2013).

However, some limitations of the procedure have been described. Grafting of frozen–thawed ovarian tissue in patients has shown limited graft life span, poor responder hormone profiles and empty follicles upon aspiration (Meirow *et al.*, 2007; Donnez *et al.*, 2008; Dolmans *et al.*, 2009). Experimental studies appear to show a decline in the primordial follicular pool (Baird *et al.*, 1999; Nisolle *et al.*, 2000), follicular activation (Dolmans *et al.*, 2007) and asynchronized development of oocyte and follicular cells (Nottola *et al.*, 2008). Further investigations are therefore required to improve the technique.

Ischemic stress is thought to be one of the factors limiting the success of the procedure (Israely *et al.*, 2004; Wu *et al.*, 2010; Friedman *et al.*, 2012). Ovarian cortical pieces are grafted without vascular anastomosis and implants are thus exposed to ischemic damage during an initial post-transplantation period until they become revascularized (Van Eyck *et al.*, 2009, 2010). During this period, profound modifications of gene regulation and physiological functions are critical for tissue survival in anaerobic conditions. However, these modifications could induce alterations in stromal tissue and deregulation of ovarian function, resulting in follicle loss and disordered follicular activation (David *et al.*, 2012). It is therefore important to understand which processes are triggered by transplantation and ischemic stress in ovarian grafts.

Multiple signaling pathways are activated in mammalian cells during ischemia/reperfusion injury in an attempt to minimize cellular injury and maintain tissue function. Among the transcriptional regulators activated are members of the hypoxia inducible factor (HIF) transcription factor family. HIF factors regulate a variety of genes that affect a myriad of cellular processes, including metabolism, angiogenesis, cell survival and proliferation, all of which are important to maintain cell viability (Ke and Costa, 2006).

All available data on transcriptional regulation in case of ischemic stress in ovarian tissue have been obtained from murine models. After autotransplantation of immature rat ovary, a huge increase in the expression of vascular endothelial growth factor (VEGF) and transforming growth factor-beta 1 (TGFβ1) was evidenced during vascular ingrowths by RNA blot hybridization (Dissen *et al.*, 1994). Similarly, Yang *et al.* (2008) showed an increase in VEGF expression in grafted immature rat ovaries 2 days after transplantation by RT–PCR and western blot. Agca *et al.* (2009) recently reported alterations in the expression of genes involved in metabolism and growth, as well as those involved in the inflammatory response after xenotransplantation of rat ovaries into mice for 12 weeks. One study performed on human fetal ovarian tissue demonstrated a sharp increase in VEGF and angiopoietin-2 expression 2 days after xenotransplantation to nude mice (Wu *et al.*, 2010).

Xenografting of human ovarian tissue to mice has proved to be an effective model to study ovarian function and follicle development *in vivo* (Van Eyck *et al.*, 2009a, b). This model is also applied to assess gonadotoxicity of treatment, evaluate the risk of reimplanting malignant cells and optimize cryopreservation and grafting protocols.

In order to better understand the factors responsible for altered development of normal-looking follicles, it is important to gather information on the transcriptional profile of frozen–thawed ovarian tissue xenografts.

Here we analyzed the impact of freeze-thawing and grafting procedures on gene expression of human ovarian tissue after 2 and 7 days of grafting to nude mice. These time points were chosen based on recent identification by electron paramagnetic resonance (EPR) of the hypoxic period before Day 5 and progressive reoxygenation thereafter (Van Eyck, 2009). Oligonucleotide microarray (Affymetrix) was applied as a tool to screen expression of thousands of genes at a time. This approach allows identification of differential expression of genes not previously described or expected to be involved in a particular process.

Materials and Methods

Experimental design

In this study, ovarian tissue was obtained from 14 patients. Each biopsy was divided into seven fragments. One fragment served as a fresh control in order to evaluate the presence of follicles. The other six fragments were slow-frozen.

Immediately after thawing (Day 0), one fragment was fixed in formol for histological examination and another was placed in TRIzol reagent (Invitrogen) for RNA extraction to control RNA quality after cryopreservation. After extraction, RNA quality was assessed using the Agilent 2100 Bioanalyzer. The four remaining fragments were grafted to the intraperitoneal cavity of two nude mice. A total of 28 mice were grafted, each mouse receiving two fragments from the same patient. The mice were euthanized on Day 2 or 7 post-transplantation.

After graft retrieval, total RNA was extracted and its quality assessed. Among the 14 pairs of mice, 4 were used for microarray analysis and RT-qPCR evaluation. The other 10 pairs of mice served for additional RT-qPCR validation of the microarray analyses. Microarray analysis was performed on ungrafted fragments and Day 7 grafts, while PCR analyses were carried out on ungrafted tissue, and Day 2 and 7 grafts.

Tissue collection and freezing

Use of human tissue for this study was approved by the Institutional Review Board of the Université Catholique de Louvain. After obtaining written informed consent, ovarian biopsies measuring 8 × 4 mm were obtained from 14 women (between 22 and 38 years of age, 26.9 ± 6.9 years) undergoing laparoscopic surgery for benign gynecologic disease. After retrieval, ovarian tissue was immersed in a solution of *N*-2-hydroxyethylpiperazine-*N*-2-ethanesulfonic acid (HEPES)-buffered modified Eagle's medium (HEPES-MEM) (MEM, Invitrogen, Carlsbad, CA, USA) and immediately transferred from the operating room to the research laboratory on ice. The medullar part was removed and each ovarian biopsy specimen was dissected into seven cortical strips of 2 × 4 mm. Freezing of the ovarian tissue strips was performed according to the method applied for ovarian tissue banking (Dolmans *et al.*, 2013). The tissue was first suspended in 800 µl of minimal essential medium (MEM)-Glutamax™ (Invitrogen) in a cryovial. This medium was then replaced with the same amount of a cryoprotective solution containing 10% dimethyl sulfoxide (Sigma, St Louis, MO, USA) and 2% human serum albumin (Sanquin, Amsterdam, the Netherlands) in Leibowitz-15 medium (Invitrogen) at 4°C. The cryovials were cooled in a programmable freezer using the following program: (i) cooled from 0°C to −8°C at −2°C/min; (ii) seeded manually by touching the cryovials with forceps pre-chilled in liquid nitrogen; (iii) cooled to −40°C at −0.3°C/min and transferred to liquid nitrogen for storage.

For thawing and cryoprotectant removal, the cryovials were exposed to room temperature for 2 min and immersed in a water bath at 37°C until the ice completely melted. To remove the cryoprotective solution, the ovarian tissue was transferred from the cryovials to Petri dishes containing MEM-Glutamax, where it was washed three times (5 min per bath).

Transplantation into nude mice

Guidelines for animal welfare were approved by the Committee on Animal Research of the Université Catholique de Louvain. The 7- to 10-week-old female mice (NMRI nu/nu, Janvier, Le Genest St Isle, France) were housed in groups of five per cage, maintained at 28°C under controlled sterile conditions, with a 12-h light/dark cycle and free access to an autoclaved pelleted diet and water.

The mice were anesthetized by injection of ketamine (75 mg/kg; Eurovet, Heusden-Zolder, Belgium) and medetomidine (1 mg/kg Domitor; Pfizer, Cambridge, MA, USA). Cortical fragments were grafted intraperitoneally as previously described by Van Eyck *et al.* (2009). A horizontal incision was made and ovarian fragments were fixed to the lower third of the parietal peritoneum with Prolene 7/0. Each mouse received two ovarian fragments. The abdominal wall and skin were then closed with 6/0 Prolene.

Anesthesia was reversed by injection of atipamezole (1 mg/kg Antisedan; Pfizer). After 2 or 7 days, the animals were euthanized by cervical dislocation and the grafts were recovered. For each mouse, one graft was fixed in formol for histological and immunohistochemical analyses and the second was transferred to TRIzol Reagent for RNA extraction.

Histological analysis

The presence of follicles was checked in fresh tissue (Day 0, $n = 14$) and after cryopreservation and grafting (Days 2 and 7, $n = 28$). For this purpose, the ovarian fragments were dehydrated, embedded in paraffin and serially sectioned (5-µm-thick sections). Every sixth slide was stained with

hematoxylin–eosin (Merck, Darmstadt, Germany) for histological evaluation; the other slides (Superfrost Plus slides; Menzel-Glaser) were kept for immunostaining.

RNA extraction and quality assessment

RNA was extracted from Day 0 fresh tissue and from Day 2 and 7 grafts.

Total RNA extraction was carried out at 4°C using TRIzol Reagent according to the protocol of Chomczynski and Sacchi (2006). Briefly, each piece of ovarian tissue was homogenized using an Ultra-Turrax T25 homogenizer (Janke and Kunkel, Brussels, Belgium) with 1 ml of TRIzol Reagent (Invitrogen). After sample lysis, 0.2 ml of chloroform (Merck) was added and the mixture was separated into three phases by centrifugation. RNA in the clear aqueous layer was carefully collected and precipitated by adding 0.5 ml of isopropanol (Merck). The RNA pellet was washed with 75% ethanol (Merck) and then redissolved in nuclease-free water. RNA samples were further purified using RNeasy Mini Kit (Qiagen, Valencia, CA, USA) according to the manufacturer's RNA clean-up protocol. RNA samples were stored at −80°C until use.

RNA concentrations were determined using a micro-volume spectrophotometer (NanoDrop ND1000, Thermoscientific). An Agilent 2100 Bioanalyzer automated analysis system (Agilent Technologies, Palo Alto, CA) was used to assess the quality (RNA integrity number) of each RNA sample. Only groups in which all three samples (Days 0, 2 and 7) had an RNA integrity number (RIN) $\geq$6.5 were included in the analysis ($n = 10$).

The RNA was divided into two for subsequent applications: microarray and PCR.

Oligonucleotide microarray

Differential gene expression in frozen–thawed human ovarian tissue was assessed before (Day 0) and after (Day 7) grafting. All experiments were performed using GeneChip Human Genome U133A 2.0 oligonucleotide arrays, which contain 22 277 probe sets representing 20 374 transcripts and variants, including 12 701 well-characterized human genes. Day 2 samples were also processed for microarray analysis, but they did not meet the Affymetrix quality control criteria.

The eight (4 Day 0 and 4 Day 7) RNA samples destined for GeneChip hybridization were processed using the RNA amplification protocol described by Affymetrix (Affymetrix Expression Manual). Briefly, purified total RNA is reverse transcribed to synthesize first-strand complementary DNA (cDNA). Thereafter, this cDNA is converted into a double-stranded cDNA template for transcription. *In vitro* transcription is then performed to produce biotin-labeled complementary RNA using Affymetrix GeneChip 3′ Amplification One-Cycle Target Labeling and Control Reagents (Affymetrix, High Wycombe). Fifteen micrograms of biotinylated RNA was thus hybridized for 16 h to Affymetrix GeneChip Human Genome U133A 2.0. Immediately following hybridization, the probe array undergoes an automated washing and staining protocol using the Fluidics Station 450 (Affymetrix), as described in the Affymetrix GeneChip Expression Analysis Technical Manual. Scanning was performed using the Affymetrix GeneChip Scanner 3000.

Microarray data analysis

Microarray data were analyzed using Bioconductor R packages. First, raw data CEL files were imported and the quality of each microarray was checked. Then, raw data were preprocessed using the RMA method and a first expression matrix was obtained. A filtering step was applied in order to remove genes with a very low expression level across all tissues [more than 75% of intensities lower than Log2(50)] or with very low expression level variation (interquartile of intensities lower than 0.3). The Limma package was used to build a linear regression model for each gene and compute its fold change between Day 0 and 7 tissues and its *P*-value. Tight control of the family-wise Type I error rate was performed using the Sidak step-down adjustment of *P*-values. All microarray data complied with MIAME standards and were submitted to the Gene Expression Omnibus.

Gene set enrichment analysis

Gene set enrichment analysis was performed to identify the list of gene ontologies and KEGG pathways modified between Days 0 and 7. This analysis was applied to the list of each gene with an adjusted *P*-value lower than 0.05 and with a fold change higher than 2.

Network enrichment analysis

To analyze microarray expression data in more depth, the Ingenuity Pathway Analysis (Ingenuity Systems) tool was used.

Biological networks of differentially expressed genes were generated using this software. Networks are shown as nodes and lines: nodes represent genes and lines represent the relationships between the genes. All lines are supported by at least one reference from the literature. The intensity of node color indicates the degree of up- (red) or down- (green) regulation. Nodes are displayed using various shapes representing the functional class of the gene product.

Quantitative PCR validation

Based on microarray results and gene and network enrichment analysis, five transcripts with a known biological function in inflammatory, angiogenic and apoptotic processes were chosen and analyzed using RT–PCR (Table I).

Relative mRNA levels of these selected transcripts after ovarian grafting were determined by RT–PCR in the 10 Day 0, 2 and 7 RNA samples (including samples analyzed by microarray). All samples were selected on the basis of the same quality criteria (presence of follicles in fresh controls and RIN $\geq$ 6.5).

Total RNA (2.5 μg) was reverse transcribed with random hexamers (Eurogentec, Seraing, Belgium) and SuperScript RT RNase H2 reverse transcriptase (Life Technologies, Gaithersburg, MD, USA).

All real-time PCR experiments were performed using the TaqMan gene expression system (Applied Biosystems, Foster City, CA, USA) with TaqMan probes, as detailed in Table I. Human glyceraldehyde-3-phosphate dehydrogenase (GAPDH) was selected as an endogenous RNA control. All PCR reactions were performed using an ABI Prism 7700 sequence detection system (Perkin-Elmer, Applied Biosystems). After an initial cDNA denaturation and Taq polymerase activation step for 10 min at 95°C, cDNA was amplified for 40 cycles of 1 min at 95°C and 1 min at 60°C. PCR was performed in duplicate for each sample and negative controls were included.

Gene transcript expression levels were calculated by subtracting the GAPDH CT value from transcript CT values (ΔCT). Relative quantitative assessment of VEGFa, matrix metalloproteinase-14 (MMP-14), interleukin-8

Table I Primer and probe references for RT–PCR analysis.

Gene symbol	Gene name	TaqMan assay ID
VEGFa	Vascular endothelial growth factor A	Hs00173626
MMP-14	Matrix metallopeptidase-14	Hs01037009
IL-8	Interleukin-8	Hs00174103
CXCR4	C-X-C motif chemokine receptor 4	Hs00607978
TGFβ1	Transforming growth factor beta 1	Hs00998133
GAPDH	Glyceraldehyde-3-phosphate dehydrogenase	Hs00266705

(IL-8), CX-cytokine receptor-4 (CXCR4) and TGFβ1 gene expression was carried out using the ΔΔCT method (Applied Biosystems User Bulletin Number 2, docs.appliedbiosystems.com/pebiodocs/04303859.pdf). Fold-change differences in the five transcripts were determined as 2^{-} (ΔCT sample − ΔCT control).

The non-parametric two-tailed Mann–Whitney *U*-test was used and a *P*-value of <0.05 was considered statistically significant. Statistical analysis was performed using SPSS 16.0 software (SPSS, Inc., Chicago, IL, USA).

Immunohistochemical staining

One section per fresh tissue sample (Day 0, $n = 10$) and one per graft (Day 7, $n = 10$) were immunostained with anti-CXCR4 antibodies (UMB2 clone, Abcam, Cambridge, UK) to localize the presence of the protein. Sections showing follicles in the previous serial section were selected for this purpose.

Tissue sections were deparaffinized in Histosafe (YVSOLAB S.A., Beerse, Belgium), hydrated in isopropanol (Merck, Darmstadt, Germany), washed briefly in water and incubated in 3% hydrogen peroxide (Merck) for 30 min to block endogenous peroxidase activity. Slides were rinsed in water and heat epitope retrieval was performed for 20 min at 96°C using tris(hydroxymethyl)aminomethane (Tris) buffer 10 mM, pH 9.0 (Merck), supplemented with ethylenediaminetetraacetic acid 1 mM and 0.1% Tween 20 (Sigma-Aldrich, Steinheim, Germany). Sections were rinsed in Tris-buffered saline (TBS)/Triton X100. Endogenous biotin was blocked using the avidin/biotin blocking kit from Vector (SP2001; Vector Laboratories, CA, USA). Non-specific reactions were blocked in normal goat serum (NGS) 10% + bovine serum albumin (BSA) 1% (Sigma-Aldrich) in TBS for 30 min at room temperature. Sections were then incubated overnight at 4°C with rabbit monoclonal anti-CXCR4 antibody (1/100, clone UMB2, Abcam) in NGS 1% + BSA 0.1% in TBS, rinsed in TBS/Triton X100, and incubated for 1 h at room temperature with anti-rabbit biotinylated secondary antibody (1/100, Dako, CA, USA). The slides were again rinsed in TBS/Triton X100 and incubated with horseradish peroxidase/streptavidin reagent (E0432, Vector). The presence of peroxidase was revealed using 3,3′-diaminobenzidine (Dako) for 10 min at room temperature. They were then rinsed in water and specimens were counterstained with Mayer's hemalum solution (Merck, Darmstadt, Germany). Tissue sections were finally dehydrated in isopropanol and Histosafe, and mounted using DPX (Prosan, Merelbeke, Belgium).

Results

Histological evaluation of ovarian tissue

As shown in Fig. 1A, the histology of frozen–thawed ungrafted ovarian tissue was similar to that of fresh tissue. In all fragments included in the study, numerous follicles were found and stromal tissue did not show any alterations.

After 2 days of grafting, an extensive necrotic area was observed mainly in the center of grafts (Fig. 1B). Despite the presence of necrosis, follicles were observed in all grafts.

After 7 days of grafting, fibrosis was found to have replaced the necrosis seen in the central part of grafts, and vessels containing red blood cells were observed throughout the fragments (Fig. 1C). Follicles were observed in all grafts recovered after 7 days.

Microarray analyses

Differential gene expression between ungrafted and intraperitoneally grafted human frozen–thawed ovarian tissue was determined using a human-specific oligonucleotide microarray targeting 20 374 transcripts. A total of 8 microarrays, including 4 ungrafted tissue samples and 4 matched grafted tissue samples, were performed. A filtering step was applied in order to remove genes with very low expression levels across all tissues or with very low expression level variation. It should be noted that most transcripts encoding factors involved in folliculogenesis showed low expression levels and were excluded by the data filtering step. After 7 days of grafting, 84 of the transcripts were highly significantly altered (adjusted *P*-value < 0.01 and fold change > 2). Among these transcripts, 35 were up-regulated and 49 down-regulated at least two-fold compared with corresponding ungrafted tissue, as detailed in Tables II and III. Strong up-regulation of several members of the MMP family (MMP-9 and MMP-14) was observed. A number of genes involved in angiogenic processes were differentially expressed between grafted and ungrafted tissue, such as placental growth factor, C-X-C chemokine receptor type 4 (CXCR4), endothelial cell-specific molecule 1 and homeobox A5 (involved in vascular remodeling). Some factors involved in neurogenic processes were found to be down-regulated after grafting, including neuron-specific gene family member 1, dystrophin, neurofascin and synaptotagmin 1.

Gene ontologies and KEGG pathway analysis

We identified functional categories that were overrepresented after 7 days of grafting compared with controls. As reported in Table IV, major biological processes were related to tissue remodeling, including secretory processes, processes associated with tissue development, cellular adhesion and response to chemical and hormonal stimuli. As shown in Table V, the most affected cellular components were those related to the extracellular matrix and granule secretion. Interestingly, the most

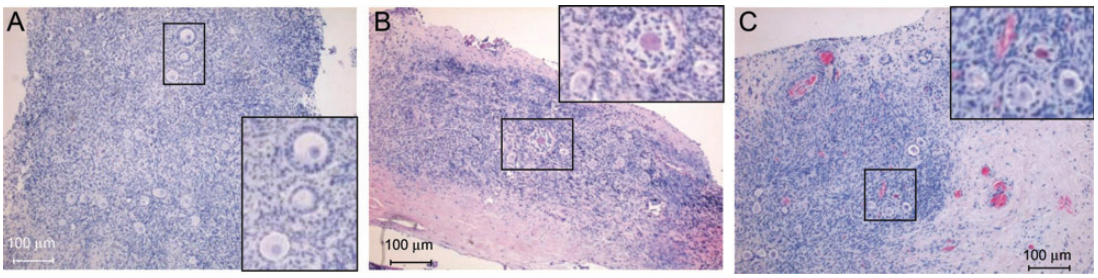

Figure 1 Histological appearance of human ovarian tissue before and after grafting for 2 and 7 days into the pelvic cavity of nude mice; (**A**) ungrafted frozen-thawed tissue with pre-antral follicles at various stages; (**B**) frozen–thawed tissue from the same patient grafted for 2 days and (**C**) for 7 days.

Table II Up-regulated gene transcripts in human ovarian tissue frozen–thawed and grafted for 7 days to the intraperitoneal cavity of nude mice compared with ungrafted tissue.

Gene title	GenBank no.	Fold change	*P*-value
Coagulation factor II (thrombin) receptor-like 1	BE965369	27.53	<0.0001
Malic enzyme 1, NADP(+)-dependent, cytosolic	L34035	22.78	0.0065
Carboxylesterase 3	NM_012122	20.74	0.0074
WNK lysine-deficient protein kinase 1	AI768512	19.94	<0.0001
GNAS complex locus	AA650558	13.73	<0.0001
Fibroblast activation protein, alpha	U76833	13.23	<0.0001
Four and a half LIM domains 1	U29538	12.95	0.0002
Kruppel-like factor 13	NM_015995	12.89	<0.0001
Matrix metallopeptidase 14 (membrane inserted)	X83535	11.89	<0.0001
Nuclear factor I/X (CCAAT-binding transcription factor)	U18759	11.81	0.0001
Cartilage intermediate layer protein	NM_003613	11.50	0.0001
Eukaryotic translation initiation factor 5A	NM_001970	11.40	<0.0001
DEAD (Asp-Glu-Ala-Asp) box polypeptide 3, X-linked	R60068	11.09	<0.0001
Prion protein 2 (dublet)	AL133396	10.15	0.0001
Matrix metallopeptidase 9	NM_004994	9.97	<0.0001
Ring finger protein 5, E3 ubiquitin protein ligase	AJ243936	9.94	0.0001
Potassium channel, subfamily K, member 3	NM_002246	8.51	0.0007
GTP-binding protein overexpressed in skeletal muscle	NM_005261	8.27	0.0003
Placental growth factor	BC001422	8.14	0.0003
Endothelial cell-specific molecule 1	NM_007036	7.62	0.0002
HOP homeobox	AB059408	7.62	0.0032
Coagulation factor II (thrombin) receptor	NM_001992	7.51	0.0006
Tumor necrosis factor, alpha-induced protein 6	NM_007115	7.42	0.0002
RNA-binding motif protein 17	NM_006450	7.32	0.0020
Chemokine (C-X-C motif) receptor 4	AJ224869	7.26	0.0006
Tumor necrosis factor, alpha-induced protein 6	AW188198	6.91	0.0003
Regulator of cell cycle	NM_014059	6.61	0.0024
ADP-ribosylation factor-like 4C	BG435404	6.37	0.0022
Cell division cycle 42 (GTP-binding protein, 25 kDa)	BC003682	6.32	0.0097
Lymphocyte antigen 6 complex, locus H	NM_002347	5.98	0.0029
Homeobox A5	NM_019102	5.86	0.0082
Striatin, calmodulin-binding protein 3	AF243424	5.69	0.0062
Aquaporin 3	N74607	5.44	0.0043
Growth-associated protein 43	NM_002045	5.41	0.0063
Thrombospondin 4	NM_003248	5.29	0.0049

significant pathways evidenced by KEGG analysis (Table VI) included metabolic pathways, such as drug metabolism/cytochrome P450 and peroxisome proliferator-activated receptor (PPAR) signaling pathways.

Ingenuity pathway analysis

To analyze gene expression data in greater depth, the Ingenuity Pathway Analysis tool was used.

The following networks were highly enriched in grafted tissue: protein synthesis, embryonic development and tissue development (enrichment score = 26); molecular transport, neurological disease, DNA replication, recombination and repair (enrichment score = 26); embryonic development, organismal development and cell signaling (enrichment score = 24); cell morphology, cellular function and maintenance and connective tissue development and function (enrichment score = 24) consistent with tissue repair and restructuring. The main network affected in grafted tissue is shown in Fig. 2, pointing to TGFβ as a key mediator of the post-grafting inflammatory response.

The top canonical pathway identified included angiopoietin signaling ($P = 5.51 \times 10^{-04}$, involving 39 genes significantly up- or down-regulated out of 74 genes included in the pathway), inhibition of angiogenesis by thrombospondin-1 ($P = 1.74 \times 10^{-03}$, involving 22 out of 39 genes), the IL-8 pathway ($P = 1.2 \times 10^{-02}$, involving 85 out of 205 genes) and PPAR activation ($P = 10^{-02}$, involving 78 out of 191 genes).

Table III Down-regulated gene transcripts in human ovarian tissue frozen–thawed and grafted for 7 days to the intraperitoneal cavity of nude mice.

Gene title	GenBank no.	Fold change	*P*-value
Heparan sulfate (glucosamine) 3-*O*-sulfotransferase 1	BF000296	0.05	0.0004
Leptin receptor	U50748	0.06	0.0003
Growth regulation by estrogen in breast cancer 1	NM_014668	0.07	0.0012
Osteomodulin	AI765819	0.07	0.0003
Hydroxysteroid dehydrogenase-like 2	BC004331	0.08	0.0003
Patched 1	BG054916	0.08	0.0004
Solute carrier family 18 (vesicular monoamine), 2	AI269290	0.08	<0.0001
Adrenoceptor alpha 2A	AF284095	0.09	0.0002
Keratin 19	NM_002276	0.10	0.0034
Family with sequence similarity 70, member A	NM_017938	0.10	0.0006
Adenylate cyclase 7	NM_001114	0.11	<0.0001
Uncharacterized LOC100507397	AW514267	0.11	0.0012
Extracellular matrix protein 2, female organ and adipocyte specific	NM_001393	0.11	0.0039
Monoamine oxidase B	NM_000898	0.12	0.0066
Acyl-CoA synthetase medium-chain family member 3	D16350	0.12	0.0004
Dehydrogenase/reductase (SDR family) member 2	AK000345	0.12	0.0003
Dpy-19-like 2 pseudogene 2 (*C. elegans*)	AL049437	0.13	0.0002
ATPase, aminophospholipid transporter, class I, 8A1	AI769688	0.13	0.0004
Glycine amidinotransferase	NM_001482	0.13	0.0011
LIM and calponin homology domains 1	AB029025	0.13	0.0005
Neurofascin	AA995925	0.14	0.0002
4-aminobutyrate aminotransferase	AF237813	0.14	0.0003
Ankyrin repeat domain 46	U79297	0.14	0.0010
K(lysine) acetyltransferase 2B	AV727449	0.14	0.0031
Insulin receptor substrate 1	NM_005544	0.14	0.0027
Secreted frizzled-related protein 1	AF017987	0.14	0.0003
LIM and calponin homology domains 1	AK026815	0.15	0.0003
Phospholipase C, epsilon 1	NM_016341	0.15	0.0011
Dystrophin	NM_004010	0.15	0.0019
Secreted frizzled-related protein 1	AF017987	0.15	0.0024
Fibronectin leucine-rich transmembrane protein 3	NM_013281	0.15	0.0083
ADAM metallopeptidase	NM_007038	0.15	0.0019
Growth factor receptor-bound protein 14	NM_004490	0.15	0.0009
Fibulin 5	NM_006329	0.15	0.0044
PDZ domain containing ring finger 3	AL569804	0.15	0.0087
Forkhead box O1	NM_002015	0.16	0.0026
Hepatic leukemia factor	NM_002126	0.16	0.0041
Hydroxysteroid dehydrogenase-like 2	AK023959	0.16	0.0010
Odd-skipped related 2 (*Drosophila*)	AI811298	0.16	0.0073
l(3)mbt-like 1 (*Drosophila*)	U89358	0.16	0.0046
Transcription elongation factor A (SII)-like 1	NM_004780	0.17	0.0078
Monoamine oxidase A	AA923354	0.18	0.0037
Uronyl-2-sulfotransferase	NM_005715	0.18	0.0049
Hepatic leukemia factor	W60800	0.18	0.0023
Neuron-specific gene family member 1	BC001745	0.18	0.0036
KIAA0895	AB020702	0.19	0.0057
Synaptotagmin I	AV731490	0.19	0.0088
Estrogen receptor 1	NM_000125	0.22	0.0195

Table IV Most modified biological functions after grafting human ovarian tissue for 7 days to the intraperitoneal cavity of nude mice.

Term	Odds ratio	Exp count	Count	Size	*P*-value
Secretion by cell	3.808	8.484	27	388	6.62E−06
Secretion	3.496	9.534	28	436	2.00E−07
Axis elongation	32.925	0.262	5	12	3.29E−07
Negative regulation of signal transduction	2.912	7.741	20	354	8.33E−07
Response to chemical stimulus	2.202	35.337	61	1616	2.75E−08
Response to hormone stimulus	3.026	9.971	26	456	5.41E−08
Anatomical structure morphogenesis	2.263	25.846	48	1182	7.46E−08
Cell adhesion	2.554	11.589	26	530	7.48E−08
Biological adhesion	2.554	11.589	26	530	7.48E−08
Tissue development	2.367	14.519	30	664	9.00E−08

List of statistically significant categories based on gene ontology (GO) annotation, sorted according to the statistical significance of their enrichment ($P < 0.01$). Size=total number of transcripts in each category. Count=number of transcripts differentially expressed between grafted and ungrafted tissue. Exp count=mean number of genes.

Table V Most modified cellular components after grafting human ovarian tissue for 7 days to the intraperitoneal cavity of nude mice.

Term	Odds ratio	Exp count	Count	Size	*P*-value
Extracellular matrix	5.69	4.708	22	228	1.29E−05
Proteinaceous extracellular matrix	5.172	3.862	17	187	2.65E−07
Extracellular region	2.616	18.441	40	893	1.33E−08
Extracellular region part	2.766	11.234	27	544	1.61E−09
Platelet alpha granule	9.586	0.888	7	43	2.43E−09
Secretory granule	4.643	2.932	12	142	3.44E−09
Plasma membrane	1.941	41.095	64	1990	4.80E−09
Cell periphery	1.934	41.983	65	2033	4.86E−09
Platelet alpha granule	48.284	0.124	3	6	0.00016

List of statistically significant categories based on gene ontology (GO) annotation, sorted according to the statistical significance of their enrichment ($P < 0.01$). Size = total number of transcripts in each category. Count = number of transcripts differentially expressed between grafted and ungrafted tissue. Exp count = mean number of genes.

Quantitative real-time PCR validation

Expression of a subset of five up-regulated genes was validated by real-time PCR quantification on samples included in the microarray analysis ($n = 4$ Day 0, $n = 4$ Day 7) and on additional samples ($n = 6$ day 0, $n = 6$ day 7). Ten Day 2 samples were also evaluated. The following gene transcripts were selected, as detailed in Table I: interleukin-8, VEGF, TGFβ1, MMP14 and CXCR4. Expression of all transcripts was normalized using GAPDH as a reference. As shown in Table VII, analysis of RT–PCR data indicates that IL-8, MMP-14 and CXCR4 were significantly overexpressed in Day 2 grafts compared with ungrafted controls, but not TGFβ1. On Day 7, overexpression was observed for IL-8, TGFβ1, MMP-14 and CXCR4 compared with ungrafted controls ($P < 0.05$), but not for VEGF. For VEGF transcripts whose overexpression was not confirmed by real-time PCR, the level of expression was highly variable.

CXCR4 immunostaining

As illustrated in Fig. 3, CXCR4 was mainly localized in endothelial cells lining blood vessels. Staining was mostly in membranes and cytoplasm. No staining was observed in granulosa cells or oocytes from primordial nor primary follicles. This pattern of immunolocalization was consistently encountered in fresh tissue and frozen–thawed Day 7 grafts.

Discussion

Using a murine xenotransplantation model, the current microarray study yields new information on genes and molecular mechanisms triggered after transplantation of human ovarian tissue. Seven days after intraperitoneal grafting, the most over-represented gene functions were related to tissue remodeling, cell adhesion, migration and vascularization.

These processes are likely to be triggered by hypoxic stress that avascular ovarian tissue grafts are subjected to before their revascularization. We indeed identified, by EPR oximetry, severe hypoxic conditions within grafts until Day 5, followed by progressive reoxygenation during the subsequent 5 days in this model (Van Eyck *et al.*, 2009).

Angiogenesis

Overexpression of key mediators of angiogenesis evidenced in the current study 7 days after transplantation appears to indicate an ongoing angiogenic process. This is consistent with the timing of ovarian tissue revascularization after grafting observed in our previous studies (Van Eyck *et al.*, 2009). Reperfusion of ovarian tissue was shown to be initiated on Day 5 by host vessels invading the graft and to be completed by Day 10 after reanastomosis with pre-existing human vessels within the graft. This implies a tightly regulated angiogenic process. Coordinated angiogenesis involves a balance between pro-angiogenic factors (such as PlGF, CXCR-4 evidenced in the current study) and their receptors with anti-angiogenic and vascular stabilizing factors (such as thrombospondin and angiopoietin pathways overexpressed in grafts).

The current study points to TGFβ, a mediator of the angiogenic response after ovarian tissue transplantation, as shown in previous studies (Dissen *et al.*, 1994; Yang *et al.*, 2008). It also confirms the involvement of angiopoietins, known to be essential for neovessel formation and maturation (Wu *et al.*, 2010). Angiopoietin-2 and its receptor were shown to be up-regulated, while angiopoietin-1 was down-regulated.

Table VI KEGG pathway analysis.

Term	KEGG ID	Odds ratio	Exp count	Count	Size	*P*-value
Glycine, serine and threonine metabolism	260	14.524	0.476	5	20	7.9E−09
Dilated cardiomyopathy	5414	5.138	1.356	6	57	0.0020
Tryptophan metabolism	380	8.175	0.595	4	25	0.0025
Intestinal immune network for IgA production	4672	7.46	0.642	4	27	0.0034
Malaria	5144	6.347	0.737	4	31	0.0057
Beta-alanine metabolism	410	9.8	0.381	3	16	0.0058
Valine, leucine and isoleucine degradation	280	5.707	0.809	4	34	0.0080
Arginine and proline metabolism	330	5.707	0.809	4	34	0.0080
Butanoate metabolism	650	8.488	0.428	3	18	0.0081
Phagosome	4145	3.289	2.379	7	100	0.0089
Leukocyte transendothelial migration	4670	3.668	1.832	6	77	0.0092
Histidine metabolism	340	7.485	0.476	3	20	0.0110
Fat digestion and absorption	4975	7.067	0.5	3	21	0.0126
Tyrosine metabolism	350	6.693	0.523	3	22	0.0144
Cell adhesion molecules (CAMs)	4514	3.246	2.046	6	86	0.0155
Propanoate metabolism	640	6.356	0.547	3	23	0.0162
Phenylalanine metabolism	360	12	0.214	2	9	0.0180
PPAR signaling pathway	3320	4.378	1.023	4	43	0.0181
GnRH signaling pathway	4912	3.463	1.594	5	67	0.0205
Drug metabolism—cytochrome P450	982	4.881	0.69	3	29	0.0303
Hypertrophic cardiomyopathy	5410	3.624	1.213	4	51	0.0318
Staphylococcus aureus infection	5150	4.698	0.714	3	30	0.0331
Rheumatoid arthritis	5323	3.403	1.285	4	54	0.0382
Lysine biosynthesis	300	41.544	0.048	1	2	0.0470
Asthma	5310	6.45	0.357	2	15	0.0480

Size=total number of transcripts in each category. Count=number of transcripts differentially expressed between grafted and ungrafted tissue. Exp count=mean number of genes.

Their coordinated expression is essential to consolidate VEGF-mediated neovessel formation and complex vascular network formation (Asahara *et al.*, 1998).

The current study also demonstrated up-regulation of angiogenesis mediators never before described in the context of ovarian tissue transplantation. Placental growth factor (PlGF), another member of the VEGF sub-family involved in angiogenic processes, was shown to be strongly up-regulated after grafting. PlGF, which is known to be induced by hypoxia and inflammation (Green *et al.*, 2001), may potentiate the mitogenic action of VEGF on endothelial cells (Park *et al.*, 1994).

Our microarray and PCR data also suggest strong up-regulation of the C-X-C chemokine receptor type 4 (CXCR4) after grafting. Immunohistochemical analysis showed strong expression of CXCR4 in endothelial cells lining blood vessels in ovarian tissue grafts. CXCR4 and its ligand, stromal-derived factor-1 (SDF-1), are strongly up-regulated under hypoxic conditions in monocytes, macrophages, stem cells and endothelial cells. The SDF-1/CXCR4 axis is an essential cell migration and adhesion signaling system, playing an important role in tissue restructuring (Schioppa *et al.*, 2003). In the current study, its vascular immunolocalization points to its involvement in neovessel formation. Activation of CXCR4 by SDF-1 was shown to induce proliferation, chemotaxis and endothelial tube formation (Heidemann *et al.*, 2004). In the neonatal murine ovary, the CXCR4/SDF-1 axis was also found to be involved in follicular development by inhibiting primordial to primary follicle transition (Holt *et al.*, 2006). However, in the current study, we did not evidence CXCR4 immunostaining in follicles in grafted or ungrafted human ovarian tissue, suggesting that CXCR4 is not implicated in human adult ovarian folliculogenesis.

IL-8 signaling was also evidenced as a prominent pathway in Day 7 grafts. Il-8 is known to be mostly expressed by macrophages, epithelial cells and endothelial cells. In the ovary, IL-8 is also expressed by granulosa and theca cells from antral follicles, modulating endothelial cell permeability during ovulation (Chang *et al.*, 1998). IL-8 was shown to act as a proangiogenic cytokine in the context of ovarian carcinoma (Merritt *et al.*, 2008). *In vitro*, IL-8 had a direct impact on endothelial cells by enhancing their proliferation and survival, and by inducing MMP-9 expression, also strongly overexpressed in Day 7 grafts (Li *et al.*, 2004). However, as a pro-inflammatory factor, IL-8 may have a negative impact after tissue transplantation by attracting neutrophils (Neri *et al.*, 2007). The IL-8 axis clearly merits further investigation in the context of ovarian physiology and grafting.

TGFβ1, another cytokine up-regulated in ovarian xenografts, plays an important role in the control of vascular function (Goumans *et al.*, 2009). It can act as a regulator of proliferation, migration, survival, differentiation

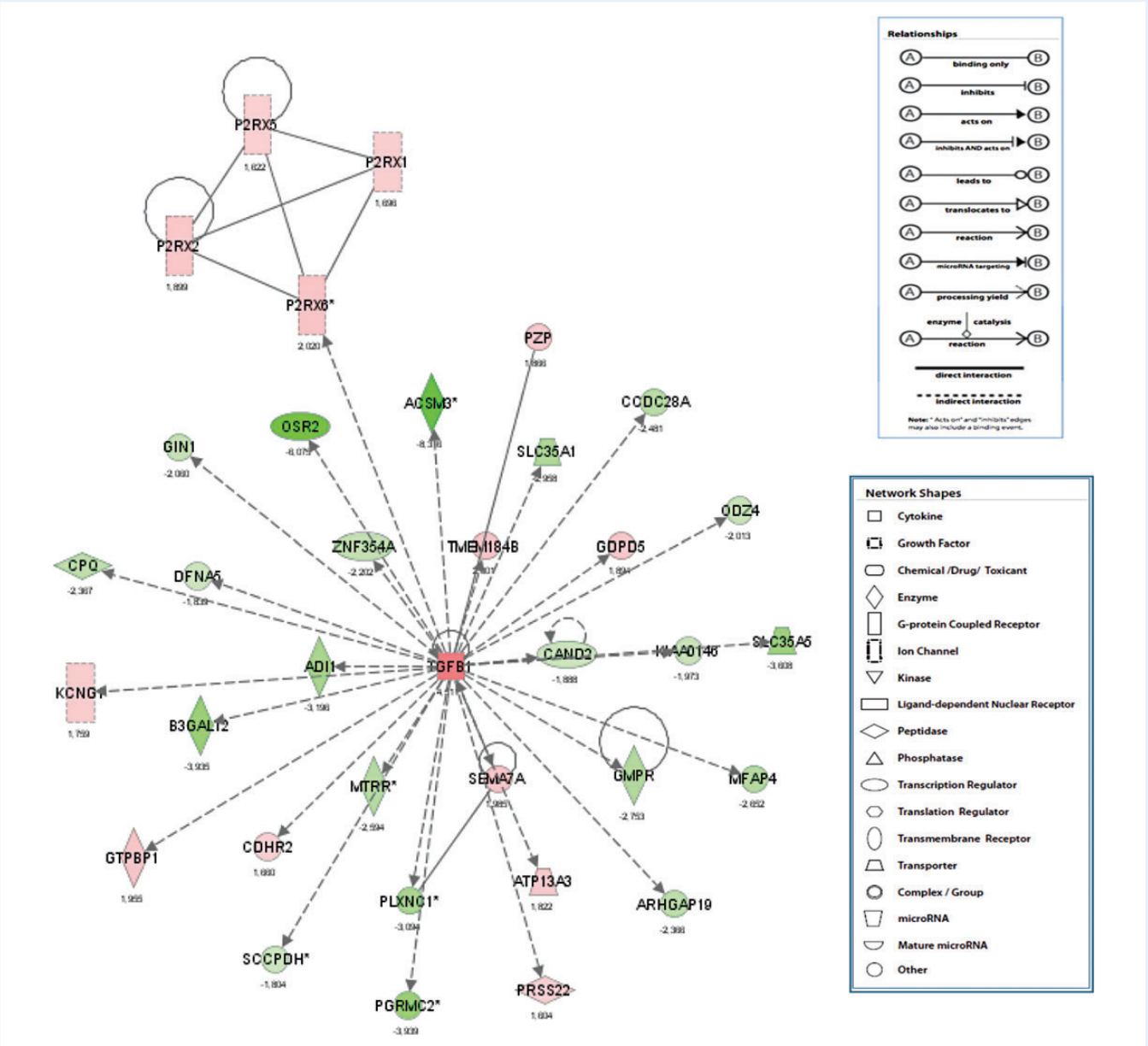

Figure 2 Main network affected in grafted versus ungrafted ovarian tissue, as evidenced by Ingenuity Pathway Analysis. Networks include nodes and lines: nodes represent genes and lines represent the relationships between the genes. All lines are supported by at least one reference from the literature. The intensity of node color indicates the degree of up- (red) or down- (green) regulation. Nodes are displayed using various shapes representing the functional class of the gene product. Gene annotations are defined in Supplementary data, Table SI.

and extracellular matrix synthesis in endothelial cells and vascular smooth muscle cells.

TGFβ1 also appears to play a key role in reproductive function, as null mutation in TGFβ1 disrupts ovarian function and causes oocyte incompetence and early embryo arrest in mice (Ingman and Robertson, 2009).

Neurogenesis

Neurogenic factors appear to be down-regulated after grafting, including neuron-specific gene family member 1, dystrophin, neurofascin and synaptotagmin I. This may be explained by a slow reinervation process after ovarian tissue grafting, in line with observations made after grafting of other tissue types, where nerves were evidenced in grafts after several months (Takahashi *et al.*, 2001).

Tissue remodeling

On Day 7 post-transplantation, several genes involved in extracellular matrix remodeling (MMP14, MMP9) are up-regulated and tissue development is among the most over-represented of gene functions. These results are in accordance with our histological observations, showing necrotic tissue 2 days after transplantation gradually replaced by fibrotic tissue by Day 7. Over time, the remnants of necrotic tissue are gradually resorbed and replaced by scar tissue. Stromal tissue damage may be

Table VII Validation of array data by real-time RT–PCR quantification.

Gene symbol	Accession	Fold change Day 2	Fold change Day 7
IL8	NM_000584	286.9[a]	56.4[a]
VEGF	AF091352	4.5	3.65
TGFβ1	BC000125	1.04	2.14[a]
MMP14	X83535	0.93[a]	7.59[a]
CXCR4	L01639	20.8[a]	10.96[a]

Data are shown as 2^{-} (ΔCT sample − ΔCT control), $n = 10$. Results were normalized using GAPDH as a control and expressed as fold increase relative to ungrafted ovarian tissue.
[a]Significantly overexpressed compared with ungrafted ovarian control tissue ($P < 0.05$, Mann–Whitney *U*-test).

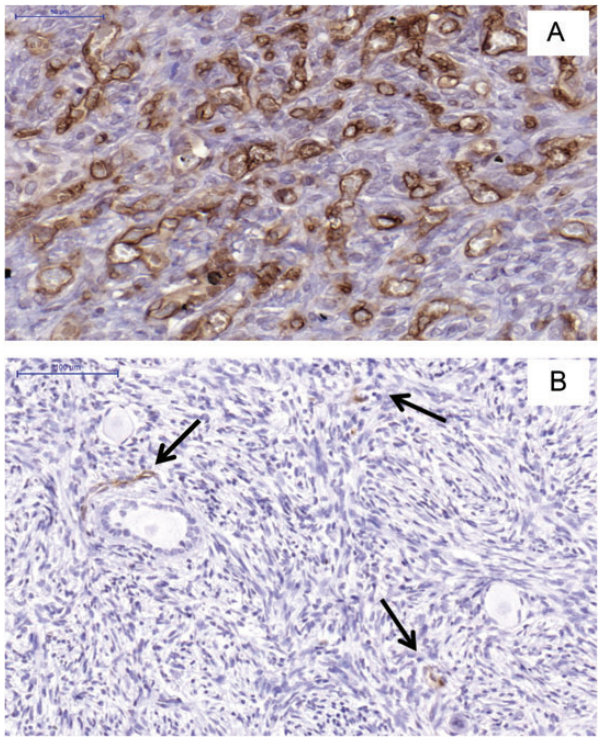

Figure 3 Representative photomicrograph showing CXCR4 immunostaining in frozen–thawed human ovarian tissue grafted intraperitoneally for 7 days to mice; (**A**) CXCR4-positive vessels (scale bar = 50 μm) and (**B**) unstained follicles and CXCR4-immunostained vessels shown by an arrow (scale bar = 100 μm).

ascribed to both the freezing process and post-transplantation ischemic stress in the interval between tissue collection and graft revascularization (Kim *et al.*, 2004; Van Eyck *et al.*, 2009).

Interestingly, extracellular proteases such as serine proteases and matrix metalloproteinases (MMPs), which were found to be strongly up-regulated after grafting, are known to play pivotal roles in physiological folliculogenesis and ovulatory processes (Rodgers *et al.*, 2003; Smith *et al.*, 2002). Under physiological conditions, the ovary undergoes cyclic remodeling of its extracellular matrix to allow growth and expansion of the follicle and breakdown and repair of the follicular wall at the time of ovulation.

Fibroblast activation protein alpha, a gelatinase of the serine protease family, also appears to be induced after grafting. Although this protein was not detected in normal ovarian tissue by immunohistochemistry (Zhang *et al.*, 2011), it was found to be overexpressed in ovarian cancer.

Extracellular matrix remodeling essential for tissue repair and revascularization may be mediated by the peroxisome PPAR pathway. This pathway was shown to be up-regulated on Day 7 after grafting using both Ingenuity and KEGG pathway analysis tools. PPARs are a family of transcription factors involved in various processes such as steroidogenesis, angiogenesis, tissue remodeling, cell cycles, apoptosis and lipid metabolism. PPARs regulate the balance of proteolytic enzymes and their inhibitors involved in tissue remodeling and angiogenesis. However, alterations in PPAR signaling may also impact on follicular development and oocyte maturation. Transgenic mice lacking PPARγ indeed showed reduced fertility (Cui *et al.*, 2002), although the mechanisms involved are poorly understood.

Interestingly, tumor necrosis factor-alpha-induced protein 6 (TGS-6) was shown to be present in ovarian tissue grafts. This hyaluronan-binding protein induced by prostaglandins is essential to maintain the integrity of cumulus–oocyte complexes (Ochsner *et al.*, 2003). Besides its role in the maintenance of extracellular matrix stability, its hyaluronan-binding domain is also known to be involved in cell migration.

Future prospects

The hypoxic conditions that human ovarian tissue is subjected to up to Day 10 after transplantation (Van Eyck *et al.*, 2010) induce profound alterations in genes associated with extracellular matrix restructuring and vascular network formation essential for tissue survival. This results in large fibrotic tissue scarring persisting in the long term, as observed in xenografts (Amorim *et al.*, 2011) as well as in patients (Camboni *et al.*, 2008), and may induce changes in the vascular network (Van Eyck *et al.*, 2010). As extracellular matrix proteins and angiogenic mediators involved in these processes after grafting are also implicated in folliculogenesis, this may account for the reduction in oocyte quality encountered in ovarian tissue grafts (Dolmans *et al.*, 2009).

It would be interesting to evaluate the consequences of ovarian tissue grafting on gene expression at the follicular level. Unfortunately, despite careful selection of biopsies containing numerous follicles, follicle markers showed low expression levels and could not be analyzed in the present study. To specifically screen the pattern of expression in follicles after grafting, enzymatic isolation (Vanacker *et al.*, 2011) or laser capture microdissection of follicles within tissue (Markholt *et al.*, 2012) may be considered.

Several strategies have been tested to reduce hypoxic stress after ovarian tissue transplantation, including addition of angiogenic factors to hasten revascularization (Shikanov *et al.*, 2011; Friedman *et al*, 2012; Labied *et al.*, 2013) and supplementation with antioxidant to reduce oxidative stress (Friedman *et al.*, 2012).

VEGF previously emerged as a promising option to precipitate recruitment of blood vessels and promote graft reperfusion in xenotransplantation models (Shikanov *et al.*, 2011; Friedman *et al*, 2012; Labied *et al.*,

2013). Expression levels of VEGF were highly variable in the current study, which highlights the importance of other mediators of the post-grafting angiogenic response that may potentiate the effect of VEGF. PlGF, as a VEGFR1-specific agonist, may act synergically with VEGF to promote neovessel formation, as demonstrated for tumor vasculogenesis in a murine model (Li *et al.*, 2009). To enhance endothelial cell recruitment, combining VEGF with SDF-1 may be considered in order to attract endothelial cells expressing CXCR4. Use of VEGF and SDF-1 together rather than individually has been proposed as a strategy to improve therapeutic neovascularization (Yu *et al.*, 2009). Concerted actions of VEGF with additional mediators, such as angiopoietins, may be beneficial to favor vessel stabilization and maturation (Thurston, 2002).

In conclusion, this study has contributed to identifying differences in gene expression after human ovarian tissue xenografting. Some of the genes have not been previously described in this tissue, so the present data provide a basis for future studies on their function and regulation. Increased knowledge of gene expression would enhance our understanding of molecular pathways involved in graft recovery and follicular development after grafting. This would allow appropriate action to be taken to improve the life span of the graft.

Acknowledgements

The authors thank Dolores Gonzalez for her technical assistance, Mira Hryniuk for reviewing the manuscript and Anne Lepage for her administrative assistance.

Supplementary data

Supplementary data are available at http://molehr.oxfordjournals.org/online.

Authors' roles

A.V.L., L.R. and J.D. designed the study; L.R. and B.B. conducted research; J.A. and L.R. analyzed data; C.A.A., M.M.D. and J.L.G. supervised the laboratory component of the study, A.V.L. and L.R. wrote the manuscript; J.D., J.L.G., C.A.A. and M.M.D. reviewed the manuscript.

Funding

This work was supported by grants from the Fonds National de la Recherche Scientifique de Belgique (grant Télévie No 7.4518.12F, grant 5/4/150/5 awarded to M.M.D.), the Fondation St Luc, the Foundation Against Cancer and donations from Mr Pietro Ferrero, Baron Frère and Viscount Philippe de Spoelberch.

References

Agca C, Lucy MC, Agca Y. Gene expression profile of rat ovarian tissue following xenotransplantation into immune-deficient mice. *Reproduction* 2009;**137**:957–967.

Amorim CA, David A, Dolmans MM, Camboni A, Donnez J, Van Langendonckt A. Impact of freezing and thawing of human ovarian tissue on follicular growth after long-term xenotransplantation. *J Assist Reprod Genet* 2011;**28**:1157–1165.

Asahara T, Chen D, Takahashi T, Fujikawa K, Kearney M, Magner M, Yancopoulos GD, Isner JM. Tie2 receptor ligands, angiopoietin-1 and angiopoietin-2, modulate VEGF-induced postnatal neovascularization. *Circ Res* 1998;**83**:233–240.

Baird DT, Webb R, Campbell BK, Harkness LM, Gosden RG. Long-term ovarian function in sheep after ovariectomy and transplantation of autografts stored at −196°C. *Endocrinology* 1999;**140**:462–471.

Camboni A, Martinez-Madrid B, Dolmans MM, Nottola S, Van Langendonckt A, Donnez J. Autotransplantation of frozen-thawed ovarian tissue in a young woman: ultrastructure and viability of grafted tissue. *Fertil Steril* 2008;**90**:1215–1218.

Chomczynski P, Sacchi N. The single-step method of RNA isolation by acid guanidinium thiocyanate-phenol-chloroform extraction: twenty-something years on. *Nat Protoc* 2006;**1**:581–585.

Cui Y, Miyoshi K, Claudio E, Siebenlist UK, Gonzalez FJ, Flaws J, Wagner KU, Hennighausen L. Loss of the peroxisome proliferationactivated receptor gamma (PPARγ) does not affect mammary development and propensity for tumor formation but leads to reduced fertility. *J Biol Chem* 2002;**277**:17830–17835.

David A, Van Langendonckt A, Gilliaux S, Dolmans MM, Donnez J, Amorim CA. Effect of cryopreservation and transplantation on the expression of kit ligand and anti-Mullerian hormone in human ovarian tissue. *Hum Reprod* 2012;**27**:1088–1095.

Dissen GA, Lara HE, Fahrenbach WH, Costa ME, Ojeda SR. Immature rat ovaries become revascularized rapidly after autotransplantation and show a gonadotropin-dependent increase in angiogenic factor gene expression. *Endocrinology* 1994;**134**:1146–1154.

Dolmans MM, Martinez-Madrid B, Gadisseux E, Guiot Y, Yuan WY, Torre A, Camboni A, Van Langendonckt A, Donnez J. Short-term transplantation of isolated human ovarian follicles and cortical tissue into nude mice. *Reproduction* 2007;**134**:253–262.

Dolmans MM, Donnez J, Camboni A, Demylle D, Amorim C, Van Langendonckt A, Pirard C. IVF outcome in patients with orthotopically transplanted ovarian tissue. *Hum Reprod* 2009;**24**:2778–2787.

Dolmans MM, Jadoul P, Gilliaux S, Amorim CA, Luyckx V, Squifflet J, Donnez J, Van Langendonckt A. A review of 15 years of ovarian tissue bank activities. *J Assist Reprod Genet* 2013;**30**:305–314.

Donnez J, Dolmans MM, Demylle D, Jadoul P, Pirard C, Squifflet J, Martinez-Madrid B, Van Langendonckt A. Livebirth after orthotopic transplantation of cryopreserved ovarian tissue. *Lancet* 2004;**364**:1405–1410.

Donnez J, Martinez-Madrid B, Jadoul P, Van Langendonckt A, Demylle D, Dolmans MM. Ovarian tissue cryopreservation and transplantation: a review. *Hum Reprod Update* 2006;**12**:519–535.

Donnez J, Squifflet J, Van Eyck AS, Demylle D, Jadoul P, Van Langendonckt A, Dolmans MM. Restoration of ovarian function in orthotopically transplanted cryopreserved ovarian tissue: a pilot experience. *Reprod Biomed Online* 2008;**16**:694–704.

Donnez J, Dolmans MM, Pellicer A, Diaz-Garcia C, Sanchez Serrano M, Schmidt KT, Ernst E, Luyckx V, Andersen CY. Restoration of ovarian activity and pregnancy after transplantation of cryopreserved ovarian tissue: a review of 60 cases of reimplantation. *Fertil Steril* 2013;**99**:1503–1513.

Friedman O, Orvieto R, Fisch B, Felz C, Freud E, Ben-Haroush A, Abir R. Possible improvements in human ovarian grafting by various host and graft treatments. *Hum Reprod* 2012;**27**:474–482.

Goumans MJ, Liu Z, ten Dijke P. TGF-beta signaling in vascular biology and dysfunction. *Cell Res* 2009;**19**:116–127.

Green CJ, Lichtlen P, Huynh NT, Yanovsky M, Laderoute KR, Schaffner W, Murphy BJ. Placenta growth factor gene expression is induced by hypoxia in fibroblasts: a central role for metal transcription factor-1. *Cancer Res* 2001;**61**:2696–2703.

Heidemann J, Ogawa H, Rafiee P, Lügering N, Maaser C, Domschke W, Binion DG, Dwinell MB. Mucosal angiogenesis regulation by CXCR4 and its ligand CXCL12 expressed by human intestinal microvascular endothelial cells. *Am J Physiol Gastrointest Liver Physiol* 2004;**286**:G1059–G1068.

Holt JE, Jackson A, Roman SD, Aitken RJ, Koopman P, McLaughlin EA. CXCR4/SDF1 interaction inhibits the primordial to primary follicle transition in the neonatal mouse ovary. *Dev Biol* 2006;**293**:449–460.

Ingman WV, Robertson SA. The essential roles of TGFB1 in reproduction. *Cytokine Growth Factor Rev*. 2009;**20**:233–239.

Israely T, Dafni H, Nevo N, Tsafriri A, Neeman M. Angiogenesis in ectopic ovarian xenotransplantation: multiparameter characterization of the neovasculature by dynamic contrast-enhanced MRI. *Magn Reson Med* 2004;**52**:741–750.

Ke Q, Costa M. Hypoxia-inducible factor-1 (HIF-1). *Mol Pharmacol* 2006; **70**:1469–1480.

Kim SS, Yang HW, Kang HG, Lee HH, Lee HC, Ko DS, Gosden RG. Quantitative assessment of ischemic tissue damage in ovarian cortical tissue with or without antioxidant (ascorbic acid) treatment. *Fertil Steril* 2004;**82**:679–685.

Labied S, Delforge Y, Munaut C, Blacher S, Colige A, Delcombel R, Henry L, Fransolet M, Jouan C, Perrier d'Hauterive S *et al.* Isoform 111 of vascular endothelial growth factor (VEGF111) improves angiogenesis of ovarian tissue xenotransplantation. *Transplantation* 2013;**95**:426–433.

Markholt S, Grøndahl ML, Ernst EH, Andersen CY, Ernst E, Lykke-Hartmann K. Global gene analysis of oocytes from early stages in human folliculogenesis shows high expression of novel genes in reproduction. *Mol Hum Reprod* 2012;**18**:96–110.

Merritt WM, Lin YG, Spannuth WA, Fletcher MS, Kamat AA, Han LY, Landen CN, Jennings N, De Geest K, Langley RR *et al.* Effect of interleukin-8 gene silencing with liposome-encapsulated small interfering RNA on ovarian cancer cell growth. *J Natl Cancer Inst* 2008;**100**:359–372.

Neri F, Puviani L, Tsivian M, Prezzi D, Pacilé V, Cavallari G, Bertelli R, Bianchi E, Piras GL, Pariali M *et al.*. Protective effect of an inhibitor of interleukin-8 (meraxin) from ischemia and reperfusion injury in a rat model of kidney transplantation. *Transplant Proc* 2007;**39**:1771–1772.

Nisolle M, Casanas-Roux F, Qu J, Motta P, Donnez J. Histologic and ultrastructural evaluation of fresh and frozen-thawed human ovarian xenografts in nude mice. *Fertil Steril* 2000;**74**:122–129.

Nottola SA, Camboni A, Van Langendonckt A, Demylle D, Macchiarelli G, Dolmans MM, Martinez-Madrid B, Correr S, Donnez J. Cryopreservation and xenotransplantation of human ovarian tissue: an ultrastructural study. *Fertil Steril* 2008;**90**:23–32.

Ochsner SA, Russell DL, Day AJ, Breyer RM, Richards JS. Decreased expression of tumor necrosis factor-alpha-stimulated gene 6 in cumulus cells of the cyclooxygenase-2 and EP2 null mice. *Endocrinology* 2003; **144**:1008–1019.

Park JE, Chen HH, Winer J, Houck KA, Ferrara N. Placenta growth factor. Potentiation of vascular endothelial growth factor bioactivity, in vitro and in vivo, and high affinity binding to Flt-1 but not to Flk-1/KDR. *J Biol Chem* 1994;**269**:25646–25654.

Rodgers RJ, Irving-Rodgers HF, Russell DL. Extracellular matrix of the developing ovarian follicle. *Reproduction* 2003;**126**:415–424.

Schioppa T, Uranchimeg B, Saccani A, Biswas SK, Doni A, Rapisarda A, Bernasconi S, Saccani S, Nebuloni M, Vago L *et al.* Regulation of the chemokine receptor CXCR4 by hypoxia. *J Exp Med* 2003;**198**:1391–1402.

Shikanov A, Zhang Z, Xu M, Smith RM, Rajan A, Woodruff TK, Shea LD. Fibrin encapsulation and vascular endothelial growth factor delivery promotes ovarian graft survival in mice. *Tissue Eng Part A* 2011; **17**:3095–3104.

Smith MF, Ricke WA, Bakke LJ, Dow MP, Smith GW. Ovarian tissue remodeling: role of matrix metalloproteinases and their inhibitors. *Mol Cell Endocrinol* 2002;**191**:45–56.

Takahashi T, Kakita A, Sakamoto I, Takahashi Y, Hayashi K, Tadokoro F, Yamashina S. Immunohistochemical and electron microscopic study of extrinsic hepatic reinnervation following orthotopic liver transplantation in rats. *Liver* 2001;**21**:300–308.

Thurston G. Complementary actions of VEGF and angiopoietin-1 on blood vessel growth and leakage. *J Anat* 2002;**200**:575–580.

Vanacker J, Camboni A, Dath C, Van Langendonckt A, Dolmans MM, Donnez J, Amorim CA. Enzymatic isolation of human primordial and primary ovarian follicles with Liberase DH: protocol for application in a clinical setting. *Fertil Steril* 2011;**96**:379–383.

Van Eyck AS, Jordan BF, Gallez B, Heilier JF, Van Langendonckt A, Donnez J. Electron paramagnetic resonance as a tool to evaluate human ovarian tissue reoxygenation after xenografting. *Fertil Steril* 2009; **92**:374–381.

Van Eyck AS, Bouzin C, Feron O, Romeu L, Van Langendonckt A, Donnez J, Dolmans MM. Both host and graft vessels contribute to revascularization of xenografted human ovarian tissue in a murine model. *Fertil Steril* 2010; **93**:1676–1685.

Wallace WH, Anderson RA, Irvine DS. Fertility preservation for young patients with cancer: who is at risk and what can be offered? *Lancet Oncol* 2005;**6**:209–218.

Wu D, Lei Y, Tong Y, Tang F, Qian Y, Zhou Y. Angiogenesis of the frozen-thawed human fetal ovarian tissue at the early stage after xenotransplantation and the positive effect of Salviae miltiorrhizae. *Anat Rec* 2010;**293**:2154–2162.

Yang H, Heun Lee H, Chang Lee H, Sung Ko D, Kim SS. Assessment of vascular endothelial growth factor expression and apoptosis in the ovarian graft: can exogenous gonadotropin promote angiogenesis after transplantation? *Fertil Steril* 2008;**90**:1550–1558.

Yu JX, Huang XF, Lv WM, Ye CS, Peng XZ, Zhang H, Xiao LB, Wang SM. Combination of stromal-derived factor-1alpha and vascular endothelial growth factor gene-modified endothelial progenitor cells is more effective for ischemic neovascularization. *J Vasc Surg* 2009;**50**:608–616.

Zhang Y, Tang H, Cai J, Zhang T, Guo J, Feng D, Wang Z. Ovarian cancer-associated fibroblasts contribute to epithelial ovarian carcinoma metastasis by promoting angiogenesis, lymphangiogenesis and tumor cell invasion. *Cancer Lett* 2011;**303**:47–55.